Article

The enhancement of overall performance of lubricating grease by adding layered double hydroxides

Li Yong,[1,2] Zhou Weidong,[3] Xue Wanan,[4] Huang Yongwang,[2] Zhang Qiang,[1] Han Jingbin[1]

1. State Key Laboratory of Chemical Resource Engineering, Beijing University of Chemical Technology, Beijing 100029, China;
2. Grease branch, Sinopec Lubricant, Co., Ltd., Binhai New Area, Tianjin 300480, China;
3. State Key Laboratory of Engines, Tianjin University, Tianjin 300350, China;
4. Guoneng Beidian Shengli Energy Co., Ltd., Xilinguole, 026000, China.

Abstract: In this paper, MgAl Layered double hydroxides (LDH) were synthesized by co-precipitation method using a colloid mill and characterized by XRD, IR and SEM. The LDHs was repeatedly tested and compared with different bearing lifetime tester in lithium base grease, and it was found that the environmental-friendly LDHs had greater performance than the traditional antioxidant, and it was the development direction of a new generation of environmental-friendly antioxidants in the future. By adding LDHs into large electric shovel greats (GRK-A) in open-pit coal mine, it can be seen by PDSC evaluation that the service lifetime of grease is extended by 20% while the overall performance of grease is not affected. With the increase of LDHs addition, the grease sample gets the greater activation energy, the stronger thermal oxidation and decomposition resistance. Comparing the energy storage modulus and flow transition index at different temperatures, it can be seen that adding the right amount of LDHs needs close attention for the system oxidation resistance and viscoelasticity. For the electric shovel grease system, the best oxidation resistance and rheological properties can be achieved by adding 2% of LDHs. The rheological viscosity-temperature curves show that the grease samples with different ratios of solid LDHs have better low-temperature properties than the mine grease.

Keywords: Layered double hydroxides; grease; antioxidant; oxidative induction time

1. Introduction

Lubricating grease is a colloid disperse system in which base stock (mineral or synthetic oil) is trapped in three dimensional network of thickener [1]. Grease has obvious advantages over lubricating oil in terms of load-bearing capacity, sealing and corrosion prevention, because grease does not flow away from the contact surface [2,3]. Friction and wear are inevitable in daily production and life, which is also the main cause of mechanical failure, and grease can play a role in reducing friction and resistance, thus improving the normal operation and durability of mechanical parts [4–6]. Antioxidant is a key additive to protect lubricating oil from oxidative deterioration. At present, at least one antioxidant is added to industrial lubricating oil to improve its oxidation stability or enhance other properties, so as to meet the harsh requirements of lubricating oil in automotive, precision bearings, construction machinery and other industrial fields [7-8]. Nowadays, countries around the world pay more and more attention to environmental protection and green development, and green chemical industry has become the trend of global chemical industry development. In recent years, due to environmental and resource problems, the promotion of new antioxidants that are green, low-cost, and high-efficiency has always been the development trend of antioxidants, but there are few reports of green antioxidants that actually realize industrial applications [9-12].

Layered double hydroxides (LDH) is a new type of 2D nanomaterial [13], compared with these traditional layered materials, which possess good thermal stability [14], non-toxic [15], and low production cost [16]. The chemical formula can be expressed as: $[M^{2+}_{1-}$

Preprints (www.preprints.org) | NOT PEER-REVIEWED | Posted: 13 April 2023 doi:10.20944/preprints202304.0288.v1

$_xM^{3+}{}_x(OH)_2]^{x+}(A^{n-})_{x/n}\cdot mH_2O$. M^{2+} and M^{3+} are divalent and trivalent metal cations, respectively; A^{n-} is the interlayer anion for charge balance. Metal cations are located at the center of the hexagonal crystal of the laminates, while the hydroxide ions occupy the apexes of the hexagonal crystal. Most of metal cations, such as Mg^{2+}, Zn^{2+}, Co^{2+}, Al^{3+}, Fe^{3+}, etc., can achieve atomic-level dispersion in the laminates of LDHs. LDH materials and their composite products have been widely reported in the field of energy storage, ion exchange, drug delivery, and flame retardant additives, etc. [17–24]. There are abundant hydroxyl groups and a large number of unsaturated coordination structures on the surface and edge of the laminate, which can react with the free radicals in the lubricating oil and effectively quench alkyl free radicals and alkoxide free radicals generated by oil heating [25].

In this paper, we prepared MgAl LDH by co-precipitation method using a colloid mill. Then, the synthetic LDHs was repeatedly tested and compared on different bearing lifetime tester in lithium base grease, and it was found that the environment-friendly LDHs had better performance than the traditional antioxidant, and was the development direction of a new generation of environment-friendly antioxidant in the future.

2. Materials and methods

2.1. Materials

$Mg(NO_3)_2\cdot 6H_2O$, $Al(NO_3)_3\cdot 9H_2O$ (analytical pure, >99.0%), NaOH (analytical pure, >96.0%), and Na_2CO_3 (analytical pure, >99.8%) were supplied by Aladdin (Shanghai). The water used in the experiment was deionized water, Base oil were supplied by SK.

2.2. Synthesis of MgAl LDH

The MgAl LDH was prepared by co-precipitation method using a colloid mill. In detail, 15.052 g $Al(NO_3)_3\cdot 9H_2O$ and 20.5128 g $Mg(NO_3)_2\cdot 6H_2O$ were dissolved in 200 mL deionized water to form a clear solution A. NaOH (7.68 g) and Na_2CO_3 (8.48 g) were dissolved in 200 mL deionized water to form solution B. Solution A and B were poured into colloid mill simultaneously with rapid rotating (3000 rpm) for 3 min; and then the colloidal suspension was transferred into a reaction kettle and crystallized at 110 ℃ for 24 h. Subsequently, the product was washed with deionized water and alcohol for several times using a centrifuge. Finally, MgAl-LDH powder was obtained after drying at room temperature.

2.3. Characterization

The chemical composition and crystal structure of the samples were analyzed by X-ray powder diffractometer (D8Discover25, Bruker, Germany). The Cu Kα ray wavelength λ=0.5416 nm and the scanning step was 0.02°. The IR spectrum of the sample was tested by infrared spectrometer. The crystal structure and particle morphology of the prepared powders were characterized and observed by scanning electron microscope (FT-20). The particle size distribution and size of samples were characterized by Laser particle size analyzer.

2.4. Tribological Experiments

The tribological performance of LDH powder materials was detected by a four-ball friction tester. The testing parameters were set at a speed of 1450 rpm, a stable applied load of 196 N and a duration time of 30 min at room temperature.

2.5. Performance of anti-oxidation and bearing lifetime

Differential scanning calorimeter (PDSC) was used to determine the oxidation stability of lubricating oils.The grease lifetime is assessed by using a high-speed bearing lifetime testing machine, and the test methods are ASTM D 3336 "Determination of the lifetime of grease in ball bearings at high temperatures" and DIN 51821-2 "Determination of the effective lifetime of rolling bearing greases FE9 method"

Preprints (www.preprints.org) | NOT PEER-REVIEWED | Posted: 13 April 2023 doi:10.20944/preprints202304.0288.v1

2.6. Viscosity-temperature property

The rheological properties of lubricating oil were tested by DISCOVERY HR-3 Rotational Rheometer. The specific operation mode of the dynamic rheology test was as follows: the initial temperature was 200 ℃, the cooling rate was 5 ℃/min, the terminal temperature was -30 ℃, the shear rate was 1.01/s, and one data point was taken every 60 s. The dynamic viscosity of four lubricating oils was measured as the temperature decreased.

3. Results and Discussion

3.1. Structural characterization of MgAl LDHs materials

3.1.1. XRD of MgAl LDHs

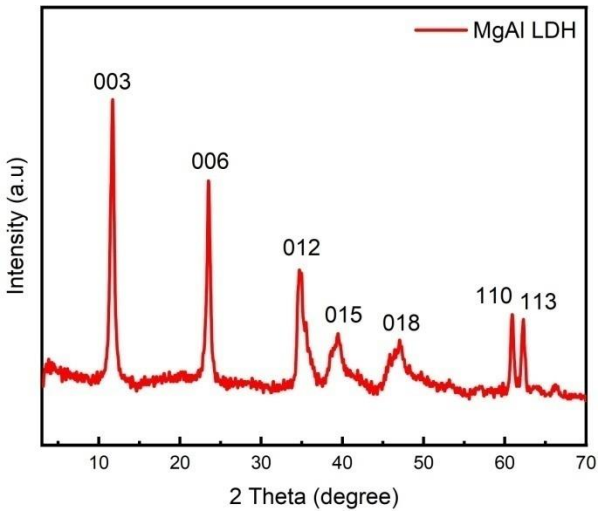

Figure 1. XRD patterns of LDH.

Figure 1 shows the XRD patterns of MgAl LDHs samples. It can be seen from the figure that the characteristic diffraction peaks of [003], [006], [009], [012], [015], [018], [110] and [113] of LDHs appear in all three samples. The diffraction peaks of the samples in the spectrogram are symmetrical and sharp, with high intensity and stable baseline, indicating that the synthesized LDHs has good crystal shape, high crystallinity and high regularity between layers. The appearance of diffraction peaks on [1010] and [1011] crystal surfaces indicates that the LDHs has fine structure. It can be seen from the position of the 003 peak that the interlayer spacing is 0.75 nm and the interlayer anion is CO_3^{2-}.

Preprints (www.preprints.org) | NOT PEER-REVIEWED | Posted: 13 April 2023 doi:10.20944/preprints202304.0288.v1

3.1.2. Fourier transform infrared spectra of MgAl-LDHs (FT-IR)

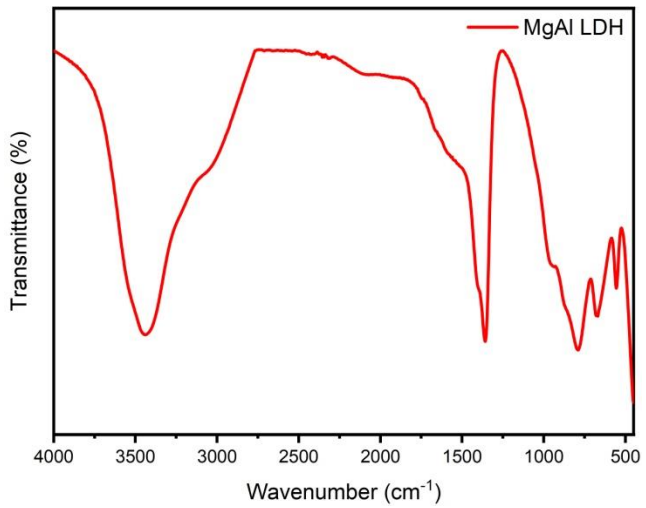

Figure 2. FT-IR spectrum of MgAl LDH.

Fourier transform infrared spectroscopy (FT-IR) was used to further study the chemical composition of MgAl LDHs (Figure 2). The wide diffraction peaks near 3480 cm^{-1} and 1657 cm^{-1} correspond to the stretching vibration absorption of -OH and the bending vibration absorption of δ-OH in LDH, respectively, and the diffraction peaks at 2960 cm^{-1} correspond to the interlaminar hydrogen bond of H_2O and CO_3^{2-}. These characteristic absorption peaks further indicate the formation of LDHs phase. The acromion at 3200 cm^{-1} is attributed to the interaction of -OH with the interlayer anion CO_3^{2-}. The diffraction peaks at 1368 cm^{-1}, 860 cm^{-1} and 660 cm^{-1} correspond to the vibration absorption of υ_2, υ_2 and υ_4 of CO_3^{2-} respectively. The diffraction peaks within 1000-500 cm^{-1} correspond to the M-O, M-O-M and O-M-O vibration absorption of LDHs skeleton. The diffraction peak at 450 cm^{-1} is attributed to the vibrational absorption of the $[AlO_6]^{3-}$ group or Al-O single bond. FT-IR results further showed that the product was MgAl-CO_3-LDH.

3.1.3. SEM image and particle size analysis of MgAl LDHs

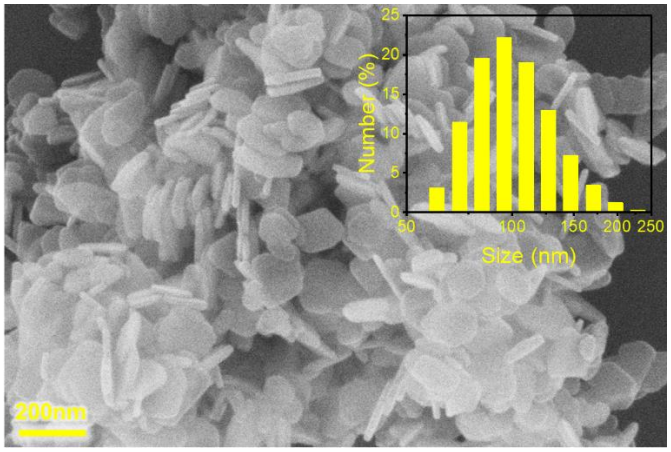

Figure 3. SEM image and particle size distribution of MgAl LDHs.

SEM figure shows that LDH prepared by co-precipitation method using a colloid mill has hexagonal sheet structure, smooth surface and sharp edge, indicating that the prepared LDHs has complete structure and high crystallinity, which is consistent with XRD characterization results. The particle size of the sample is mainly concentrated at 70-200 nm, with the average particle size $d_{0.5}$ = 100 nm. The particle size of MgAl LDH samples

Preprints (www.preprints.org) | NOT PEER-REVIEWED | Posted: 13 April 2023 doi:10.20944/preprints202304.0288.v1

prepared by co-precipitation method using a colloid mill is nano scale, with small particle size, high crystallinity and complete crystal shape. The average particle size is about 120 nm.

3.2. Study on properties of LDHs in grease

3.2.1. Study on oxidation resistance of LDHs in lithium base grease

Over the years, many oxidation bench tests have been developed and proved to be very effective for grease formulation selection, especially in the screening and formulation development of new antioxidants. Due to the limitations of the test site, a single test cannot simulate the real working conditions. Therefore, when examining grease formulation and antioxidant screening, an effective method is to use multiple test methods for comparative evaluation.

Bearing lifetime refers to the ability of grease to lubricate high temperature and high speed ball bearings for extended periods of time under light load conditions. The test method is ASTM D 3336 "*Life of Lubricating Greases in Ball Bearings at Elevated Temperatures*".

To test the lifetime of the bearing, a set of steps are undertaken. Firstly, a 3.2 ml sample is loaded into the cleaned 6204 bearing, following which the test bearing, support bearing, and finger spring are installed onto the main shaft, and the thermocouple is positioned and fixed carefully. Secondly, the device is turned on to raise the temperature of the bearing up to the measured temperature. At a speed of 10000 r/min, the bearing is run continuously until either the grease sample fails or the specific running time is achieved. The running time (in hours) is then recorded as the lifetime of the specimen in the ball bearing.

Analyzing the data presented in Tables 1 and 2, it is evident that at a temperature of 149 ℃, the bearing life of the grease sample is similar when the base grease is added with LDHs and diphenylamine at a concentration of 0.3%. Conversely, when the base grease was added with LDHs and T531 at a concentration of 0.5%, it was observed that the bearing life of the grease sample 4 (with added LDHs) doubled in comparison to sample 3 (with added T531). This indicates that the bearing life is heavily influenced by the addition of different types of antioxidants. Furthermore, these results suggest that LDH could potentially replace traditional organic antioxidants and pave the way towards sustainable, green development.

Table 1. Proportion of LDHs in general lithium base grease.

Sample	Sample 1	Sample 2	Sample 3	Sample 4
Base Oil	92.7%	92.7%	92.5%	92.5%
Soap content in grease	7%	7%	7%	7%
LDHs	0	0.3%	0	0.5%
Diphenylamine	0.3%	0	0	0
T531	0	0	0.5%	0

Table 2. Bearing lifetime test of LDHs in general lithium base grease.

Sample	Sample 1	Sample 2	Sample 3	Sample 4
CRC lifetime (149℃)	14 h	14.8 h	19.5 h	41.7 h

Table 3 and Table 4 show the results of the bearing lifetime tester test conducted by a different company, which found that the samples containing LDHs had significantly higher bearing lifetimes compared to the base grease. The base grease had a bearing lifetime of 40 hours at 149 °C. However, adding 1% of LDHs increased the grease lifetime by a factor of three, and increasing the LDH content to 3% extended the lifespan by approximately four times. Further, adding 5% of LDHs increased the grease lifetime by nearly five times. Table 6 reveals that samples 1-4 used mineral oil, while samples 5-8 used a

Preprints (www.preprints.org) | NOT PEER-REVIEWED | Posted: 13 April 2023 doi:10.20944/preprints202304.0288.v1

higher viscosity semi-synthetic oil, resulting in a significant improvement in the CRC bearing life test.

Table 3. Formulas of different proportions of LDHs general lithium base grease.

Sample	Sample 5	Sample 6	Sample 7	Sample 8
Base Grease	100%	99%	97%	95%
LDHs	0	1%	3%	5%

Table 4. ASTM D 3336 bearing lifetime test of LDHs in general lithium base grease.

Sample	Sample 5	Sample 6	Sample 7	Sample 8
CRC lifetime (149℃), h	40	120	157	188

The FE9 method is a testing process that uses angular contact ball bearings in a specialized rolling bearing grease tester to determine the effective service lifetime of grease. This test method is defined by the DIN 51821-2 standard titled "Testing of lubricants - Test using the FAG roller bearing grease testing apparatus FE9 - Part 2: Test method". The FE9 test steps involve filling five sets of clean test bearings with a certain amount of grease to be tested, and then installing these test bearings onto five test units. The test conditions are set in accordance with specific requirements, including a speed of 6000 r/min, axial force of 1500 N, and a temperature range of 120 ℃ to 220 ℃ (set as an integer multiple of 10 ℃) under test conditions. The heating system is activated to control the temperature using a temperature controller. During the test, the friction torque of the bearing will increase as a result of poor lubrication. If this results in the power of the driving motor exceeding the limit value and lasting for 6 s to 8 s, the test is ended. After the test, running times of each of the five test bearings are inputted into Weibull distribution data evaluation software to produce life failure probability distribution diagrams. The effective lifetime of the grease can be determined by reading the running time at the 50% failure probability mark on the diagram.

Through the test results in Table 3 and Table 5, it is found that the lifetime of FE9 bearings of the three samples added with LDHs are obviously better than those of the base grease, and with the increase of the amount of LDHs added, the bearing lifetime tends to increase regularly.

Table 5. DIN 51821-2 bearing life test of LDHs in general lithium base grease.

Sample	Sample 5	Sample 6	Sample 7	Sample 8
lifetime (177℃), h	77	90	107	116

Table 6. The typical properties of eight greases.

	Sample 1	Sample 2	Sample 3	Sample 4	Sample 5	Sample 6	Sample 7	Sample 8
Thickener type	lithium calcium mixed soap					lithium soap		
Base oil type	mineral oil					Semi synthetic oil		
Base oil viscosity (100℃), cst	6					8		
Cone penetration (25℃)	257	256	253	255	258	255	252	250
Drop point(℃)	185	186	182	190	193	193	193	195

3.2.2. Study on oxidation resistance of LDHs in grease for mine electric shovel

After the 1930s, electricity replaced other forms of power and became the only power of mining excavators, and the steam shovel was replaced by the electric shovel. At this time, the shovel is mainly used for stripping mining, and the large mining shovel used for stripping is called stripping shovel. With the expansion of the scale of open-pit mining,

Preprints (www.preprints.org) | NOT PEER-REVIEWED | Posted: 13 April 2023 doi:10.20944/preprints202304.0288.v1

the stripping shovel is developing towards large scale. In the 1970s, as surface mining technology improved, smaller pick-up shovels gradually replaced larger stripper shovels for easier matching with mining trucks. So far, this type of electric shovel is still the main equipment for open-pit mining mines.

At the end of 2005, the WK-20 20 m^3 electric shovel of Taiyuan Heavy Industry Co., Ltd (TYHI) was successfully launched, breaking the long-term monopoly of American companies in the field of large mining electric shovels with a bucket capacity of more than 20m^3. Since then, TYHI has developed WK-27, WK-35, WK-55 and WK-75 shovel, among which THE WK-75 shovel design standard bucket capacity of 75 m^3, is the largest type of shovel independently developed in China.

Shovel is one of the most important equipment in open-pit mining technology. Lubrication of gear mechanism of shovel has always been a difficult problem. Improper selection of lubricant often causes serious pitting corrosion, abrasion, scratch, excessive wear and other phenomena, which makes the gear enter overhaul before its service lifetime and increase the maintenance cost. It is the bounden duty of SINOPEC to prolong the use of grease in mine shovel and reduce the surface pollution caused by exposed grease in open pit coal mine.

3.2.2.1. Research on antioxidation of electric shovel grease

According to Table 7, Table 8 and Figure 4, LDHs added to shovel grease can prolong the service lifetime of grease while the overall performance of grease is not affected.

Table 7. Formula of LDHs in shovel grease.

Sample	Sample 9	Sample 10	Sample 11	Sample 12
GRK-A	100%	98%	96%	94%
LDHs	0	2%	4%	6%

Table 8. Typical product data table.

Project	Sample 9	Sample 10	Sample 11	Sample 12	Experimental method
Extreme pressure performance，PD value/N	4903	4903	4903	4903	ASTM D2596
Wear protection, scar diameter, mm, max	0.65	0.62	0.63	0.61	ASTM D2266
anticorrosive (52 ℃,48 h)	Pass	Pass	Pass	Pass	ASTM D1743
corrosion(T_2Cu,100 ℃,24h)	Pass	Pass	Pass	Pass	ASTM D4048
PDSC (190 ℃)/min	31.0	37.2	39.5	42.6	ASTM D5483

Preprints (www.preprints.org) | NOT PEER-REVIEWED | Posted: 13 April 2023 doi:10.20944/preprints202304.0288.v1

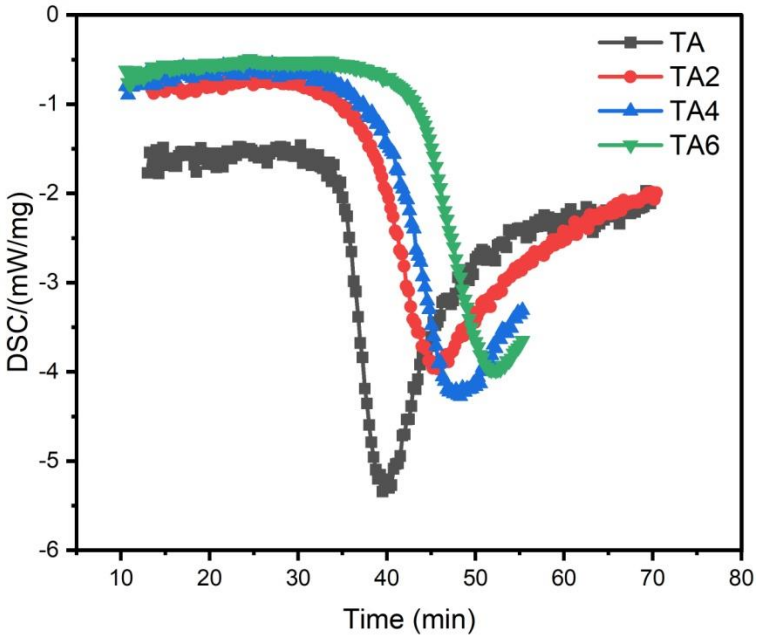

Figure 4. PDSC measurements of TA, TA2, TA4 and TA6 (Note: sample 9 is TA, sample 10 is TA2, sample 11is TA4, and sample 12 is TA6).

The main premise of DSC to study reaction kinetics is that the degree of reaction is proportional to the thermal effect released or absorbed by the reaction, that is, it is proportional to the area under the DSC curve. Can be expressed by the following formula:

$$\alpha = \frac{H}{H_T} = \frac{S_s'}{S_s}$$

$$1 - \alpha = \frac{H_T - H}{H_T} = \frac{S_s - S_s^{'}}{S_s} = \frac{S_s^{''}}{S_s}$$

$$\frac{d\alpha}{\mathrm{dt}} = \frac{1}{H_T}\frac{dH}{dt}$$

where H - enthalpy, heat of reaction at temperature T; H_T - total enthalpy of the reaction. Thus, the basic kinetic equation of the reaction can be rewritten as,

$$\frac{1}{H_T}\frac{dH}{dt} = Ae^{-\frac{E}{RT}}\left(\frac{H_T - H}{H_T}\right)^n$$

On both sides of the exponential,

$$\frac{\Delta ln\frac{dH}{dt}}{\Delta ln\,(H_t - H)} = \frac{\left(\frac{E}{R}\right)\Delta\, 1/T}{\Delta ln\,(H_t - H)} + n$$

By comparing DSC scanning curves with the same change rates of the two reactions at different rates, the activation energy E can be obtained:

$$\left[\frac{\Delta ln\frac{dH}{dt}\,\frac{1}{H_T}}{\Delta\frac{1}{T}}\right]_n = -\frac{E}{R}$$

If the change rate α is the same at peak temperature, it is further expressed as:

$$\frac{\Delta ln\frac{\beta}{T^2}}{\Delta\frac{1}{T}} = -\frac{E}{R}$$

Preprints (www.preprints.org) | NOT PEER-REVIEWED | Posted: 13 April 2023 doi:10.20944/preprints202304.0288.v1

As can be seen from Table 9-10 and Figure 5-6, the activation energies of the four samples all meet the increasing law of $E_{TA} < E_{TA2} < E_{TA4} < E_{TA6}$, indicating that with the increase of the amount of LDHs added, the larger the reaction activation energy of grease indicates the stronger its thermal anti-oxidation and decomposition ability.

Table 9. PDSC situation of samples with different heating rates.

	Warming rate β, K/min	T_{on}, ℃	T_p, ℃	T_p, K	1000/T_p, 1/K	ln(β/T^2)
Sample 9	10	236.51	240.43	513.58	1.947	-10.180
	12	238.75	241.24	514.39	1.944	-10.001
	15	240.85	246.22	519.37	1.925	-9.797
	20	252.09	260.26	533.41	1.875	-9.563
Sample 10	10	238.93	243.4	516.55	1.936	-10.192
	12	238.39	244.04	517.19	1.934	-10.012
	15	243.97	250.55	523.7	1.909	-9.814
	20	247.96	253.95	527.1	1.897	-9.539
Sample 11	10	236.16	240.84	513.99	1.946	-10.182
	12	237.16	243.4	516.55	1.936	-10.009
	15	241.56	248.37	521.52	1.917	-9.805
	20	244.71	250.83	523.98	1.908	-9.527
Sample 12	10	235.19	239.45	512.6	1.951	-10.176
	12	237.31	241.81	514.96	1.942	-10.003
	15	240.92	246.04	519.19	1.926	-9.796
	20	247.35	248.85	522	1.916	-9.520

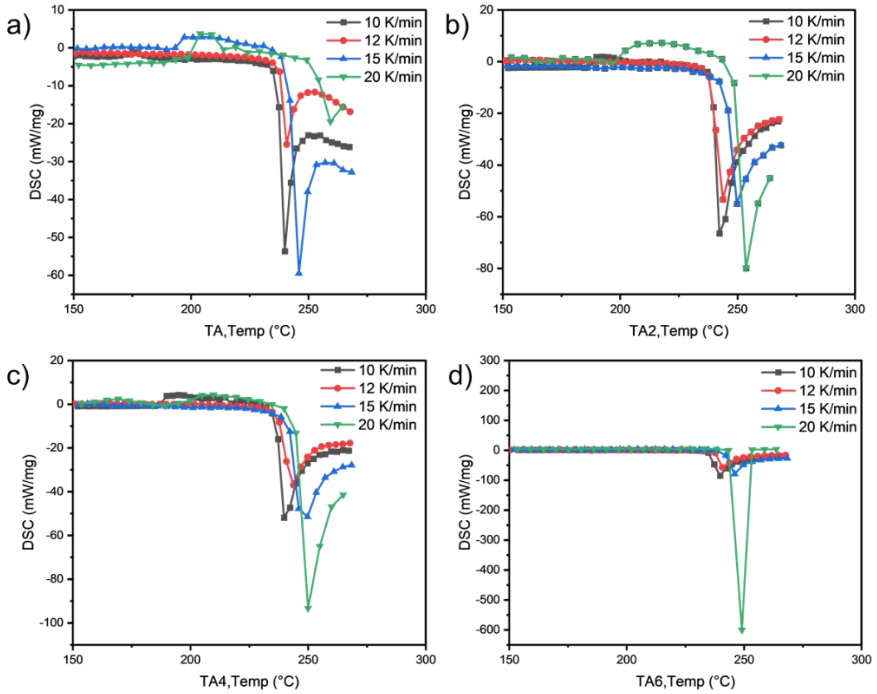

Figure 5. PDSC curves of TA, TA2, TA4 and TA6 at different heating rates.

Preprints (www.preprints.org) | NOT PEER-REVIEWED | Posted: 13 April 2023 doi:10.20944/preprints202304.0288.v1

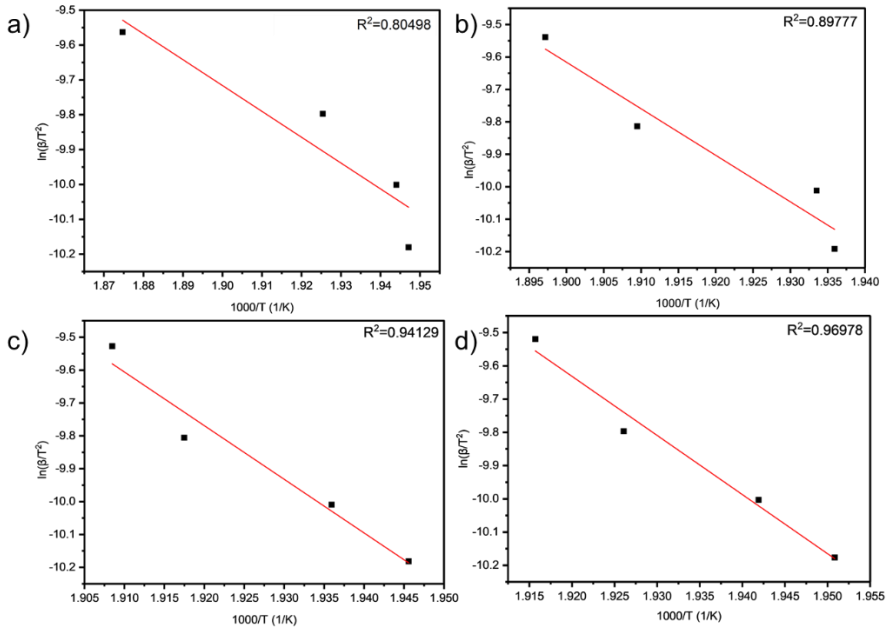

Figure 6. Linear fit results of TA/ TA2/ TA4/ TA6 were obtained using PDSC analysis.

Table 10. Correlation coefficients of different samples R^2, activation energy.

Sample	Sample 9	Sample 10	Sample 11	Sample 12
R^2	0.8049	0.8978	0.9413	0.9698
Activation energy， KJ/mol	61.61	119.24	135.68	147.87

3.2.2.2. Analysis of rheological properties of electric shovel grease

Grease is a viscoelastic non-Newtonian fluid. The elastic part of viscoelasticity is represented by the energy storage modulus G', which indicates that the stress energy can be temporarily stored and recovered during the experiment. The viscous part is represented by the loss modulus G", which indicates that the grease loses energy during the initial flow, which is converted into shear heat, and the loss is irreversible. When rheological experiments are performed, the shear stress increases, and the point where the energy storage modulus G' begins to decrease is usually defined as the end of the linear viscoelastic zone (LVE), called the yield point, and the shear stress at this point is also called the yield stress τ_y. The maximum elastic deformation that the grease can withstand can be determined by this point. Shear stress and deformation continue to increase, G' line and G"line intersection, the intersection point is called the flow point (Flow point), the shear stress at this point is called the flow stress τ_f, at this time the grease thickener structure is more damaged, the grease began to flow.

The oscillatory rheological experiments were performed on four grease samples using the method. Figure 7 shows the relationship between the storage modulus G' and loss modulus G"with the variation of shear deformation γ at different temperatures measured by changing the experimental temperatures (60, 80, 100 and 120 °C)

Preprints (www.preprints.org) | NOT PEER-REVIEWED | Posted: 13 April 2023 doi:10.20944/preprints202304.0288.v1

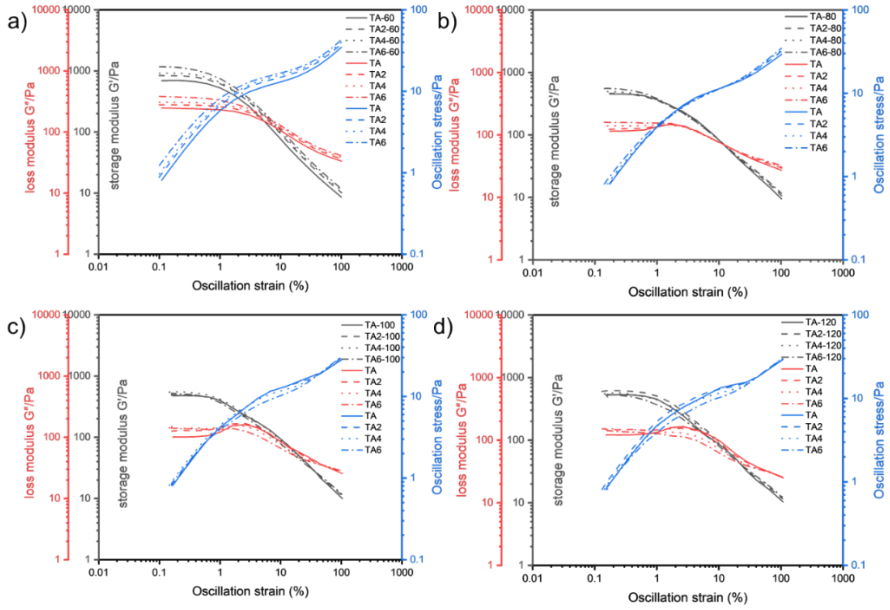

Figure 7. Variation of storage modulus, loss modulus and Oscillation stress with strain at different temperatures: (a) 60 ℃, (b) 80 ℃, (c)100 ℃, (d)120 ℃.

It can be seen from Figure 7 that the overall pattern of energy storage modulus G' of the four greases entering the rheological transition zone at 60, 80, 100 and 120 °C is gradually decreasing with the increase of temperature. From the previous principle analysis, it is known that the larger the G' is, the better the structure of the grease is maintained before it is in gel state, and the lubricating performance of the grease inside the electric shovel gear is often carried out within a few seconds after the start of operation. Therefore, it is beneficial to improve the lubrication of gears by appropriately improving the energy storage modulus and fluidity performance of grease. At 60 °C, as the proportion of LDHs increases, the energy storage modulus of TA-6 grease sample is the largest, and TA-2 is the second at 120 °C, as the proportion of LDHs increases, the energy storage modulus of TA-6 grease sample is the largest, and TA-4 is the second; at 100 °C, the energy storage modulus of TA-4 grease sample is the largest, and TA-2 is the second; at 120 °C, the energy storage modulus of TA-2 grease sample is the largest, TA is the second largest and TA-6 is the smallest; it means that at low temperature, the energy storage modulus of grease increases simultaneously with the increase of LDHs ratio, and with the increase of temperature, the larger the LDHs ratio is, the larger the system elastic deformation damage is, so it is necessary to consider the effect of suitable ratio of LDHs on energy storage modulus. Combined with the flow transition index and energy storage modulus in different linear viscoelastic intervals, it can be seen that adding two percent of LDHs is the best for the system elastic deformation and energy storage modulus. It indicates that the internal structure of sample TA-2 is more stable under shear, and the fiber structure is better maintained, which is better for gear support and lubrication, and is conducive to reducing gear wear.

The values of energy storage modulus and loss modulus, shear stress and corresponding strain values of the four greases at yield point and flow point at the two sets of experimental temperatures can be calculated and the numerical results are listed in Table 11.

Preprints (www.preprints.org) | NOT PEER-REVIEWED | Posted: 13 April 2023 doi:10.20944/preprints202304.0288.v1

Table 11. G' and G″ about four greases at yield point and critical strains corresponding to the flow point.

Samples	t/°C	yield point				flow point			τ_f/τ_y
		G′ /Pa	G″ /Pa	γ /%	τ_y/Pa	G′ （G″ ）/Pa	γ /%	τ_f	
TA	60	613.99	236.31	0.62	4.11	148.04	5.5509	11.50	2.798
	80	423.44	120.19	0.63	2.76	101.59	8.0331	10.65	3.859
	100	457.66	106.39	0.63	2.95	130.49	6.6947	11.49	3.895
	120	507.12	125.47	0.63	3.28	113.90	6.6787	11.25	3.430
TA2	60	791.08	275.02	0.63	4.87	175.96	5.5756	13.31	4.046
	80	411.87	129.02	0.63	2.72	55.62	15.6308	12.86	4.730
	100	459.57	130.17	0.63	3.00	75.75	12.9248	13.35	4.450
	120	571.78	144.25	0.63	3.11	51.35	18.4844	14.13	4.543
TA4	60	773.71	295.00	0.63	5.25	167.96	6.1426	14.39	2.741
	80	426.57	140.67	0.63	2.85	53.30	16.1876	12.89	4.523
	100	492.54	138.28	0.63	3.24	46.35	20.3598	13.81	4.262
	120	492.16	144.51	0.63	3.22	52.64	17.5229	12.90	4.006
TA6	60	903.04	351.65	0.64	6.20	140.73	8.4815	16.25	2.621
	80	460.45	155.40	0.63	3.09	58.57	14.9034	12.79	4.139
	100	447.03	134.49	0.63	2.94	45.28	19.3143	12.63	4.296
	120	441.75	131.10	0.64	2.93	50.02	17.5491	12.03	4.106

Table 11 shows that: at 60 °C, the yield point energy storage modulus G' is ranked as G'(TA-6) > G'(TA-2) > G'(TA-4) > G'(TA); at 80 °C, G'(TA-6) > G'(TA-4) > G'(TA) > G'(TA-2); at 100 °C, G'(TA-4) > G'(TA-2) > G'(TA) > G'(TA6); at 120 °C, G'(TA-2) > G'(TA) > G'(TA4) > G'(TA6);

At the flow point, the strain amplitude γ is ordered as follows: 60 °C, γ(TA-6) > γ(TA-4) > γ(TA-2) > γ(TA); 80 °C, γ(TA-4) > γ(TA-2) > γ(TA-6) > γ(TA); 100 °C, γ(TA-4) > γ(TA-6) > γ(TA-2) > γ(TA); 120 °C, γ(TA-2) > γ(TA-6) > γ(TA-4) > γ(TA);. The energy storage modulus G' is ordered as follows: 60 °C, G' (TA-2) > G' (TA-4) > G' (TA) > G' (TA-6); 80 °C, G' (TA) > G' (TA-6) > G' (TA-2) > G' (TA-4); 100°C, G' (TA) >G' (TA-2) > G' (TA-4) > G' (TA-6); 120 °C, G' (TA) > G' (TA-4) > G' (TA-2) > G' (TA-6). The shear stress τ_f is sorted as follows: 60 °C, τ_f (TA-6) > τ_f (TA-4) > τ_f (TA-2) > τ_f (TA); 80 °C, τ_f (TA-4) > τ_f (TA-2) > τ_f (TA-6) > τ_f (TA); 100 °C, τ_f (TA-4) > τ_f (TA-2) > τ_f (TA-6) > τ_f (TA); 120 °C, τ_f (TA-2) > τ_f (TA-4) > τ_f (TA-6) > τ_f (TA);.

At the flow point, the flow transition index τ_f/τ_y is ordered as follows: τ_f/τ_y(TA-2) > τ_f/τ_y(TA) > τ_f/τ_y(TA-4) > τ_f/τ_y (TA-6) for 60 °C; τ_f/τ_y(TA-2) > τ_f/τ_y(TA-4) > τ_f/τ_y(TA-6) > τ_f/τ_y (TA) for 80 °C; τ_f/τ_y (TA-2) > τ_f/τ_y(TA-6) > τ_f/τ_y(TA-4) > τ_f/τ_y(TA) for 100 °C; τ_f/τ_y(TA-2) > τ_f/τ_y(TA-6) > τ_f/τ_y(TA-4) > τ_f/τ_y (TA) for 120 °C.

The maximum value of τ_f/τ_y for sample TA-2 at the test temperature indicates that at this temperature, TA-2 grease-like soap fibers have the best structural stability and the soap fibers are less likely to fracture or break. Comparing the storage modulus and flow transition index at different temperatures, it can be seen that the addition of the appropriate amount of LDHs for the system oxidation resistance and viscoelasticity requires close attention. For the electric shovel grease system adding 2 % of LDHs can achieve the best oxidation resistance and rheological properties.

Since grease is a non-Newtonian fluid, curve fitting in this paper refers to the streamlining of flow curves of varying graphical complexity into an equation with two, three or four coefficients. Curve fitting has the following advantages: in quality control, it is easier to mathematically set the tolerance range with the help of standard regression coefficients, and it is more difficult to visually compare the shape difference between the unique flow curve formed by the measured test point and the standard curve. After completing the procedural processing of the experimental data, the second step is obviously to continue the automatic evaluation of the samples for compliance with the technical specifications. Regression calculations help to solve this problem.

These data were not fitted to the Ostwald-de-Waele model (Equation (1)) because of R^2. These presented a value of n not close to 1, as was expected for not Newtonian fluids.

Preprints (www.preprints.org) | NOT PEER-REVIEWED | Posted: 13 April 2023 doi:10.20944/preprints202304.0288.v1

The existence of a yield stress value can be recognized in Fig. 8, and the data were not satisfactorily fitted to a Herschel-Bulkley model (Equation (2)) and the results are collected in Table 12.The data were satisfactorily fitted to a Polynomial model (Equation (3), R^2>0.999) and the results are collected in Table 12.

$$\tau = A^* \gamma^n \quad (1)$$

$$\tau = \tau_0 + A^* \gamma^n \quad (2)$$

$$\tau = \tau_0 + B1^* \gamma + B2^* \gamma^2 + B3^* \gamma^3 + B4^* \gamma^4 \quad (3)$$

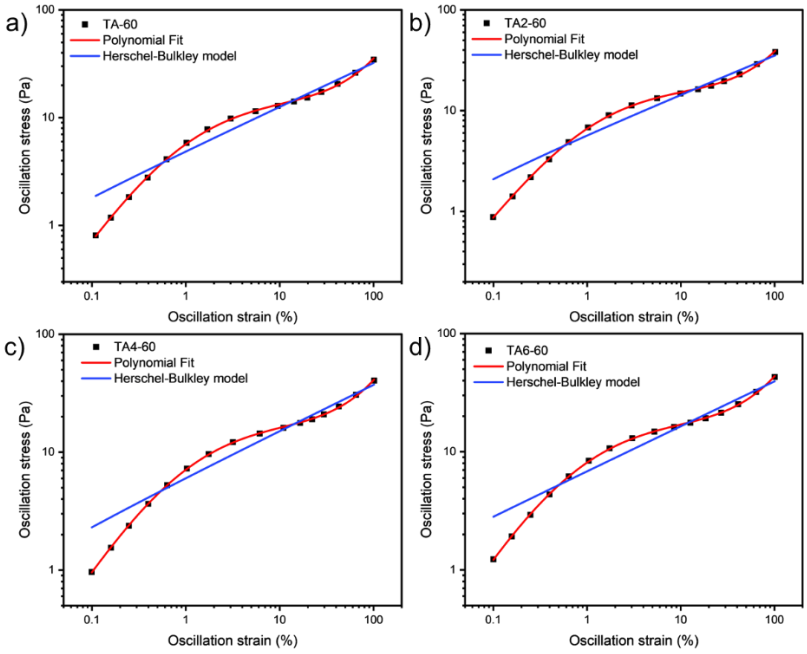

(A)

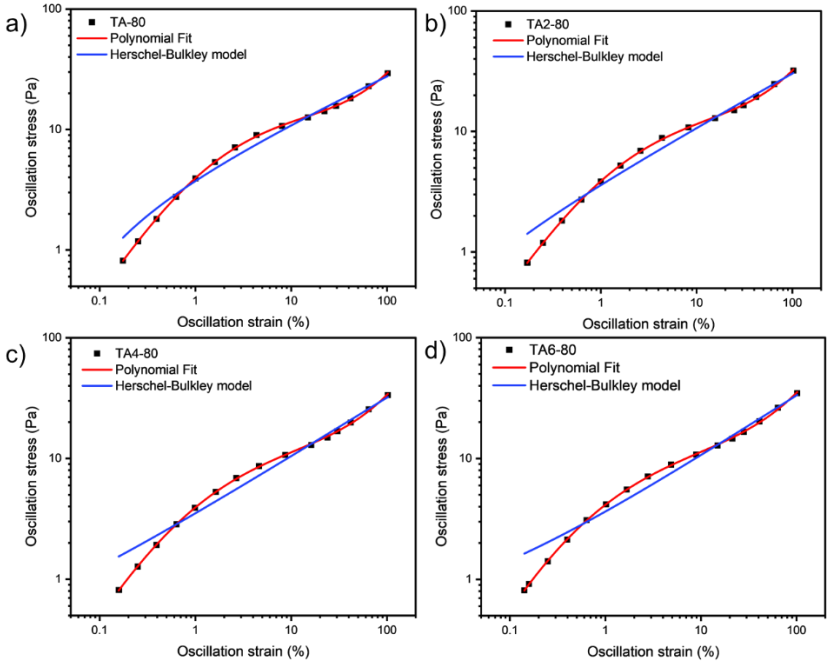

(B)

Preprints (www.preprints.org) | NOT PEER-REVIEWED | Posted: 13 April 2023 doi:10.20944/preprints202304.0288.v1

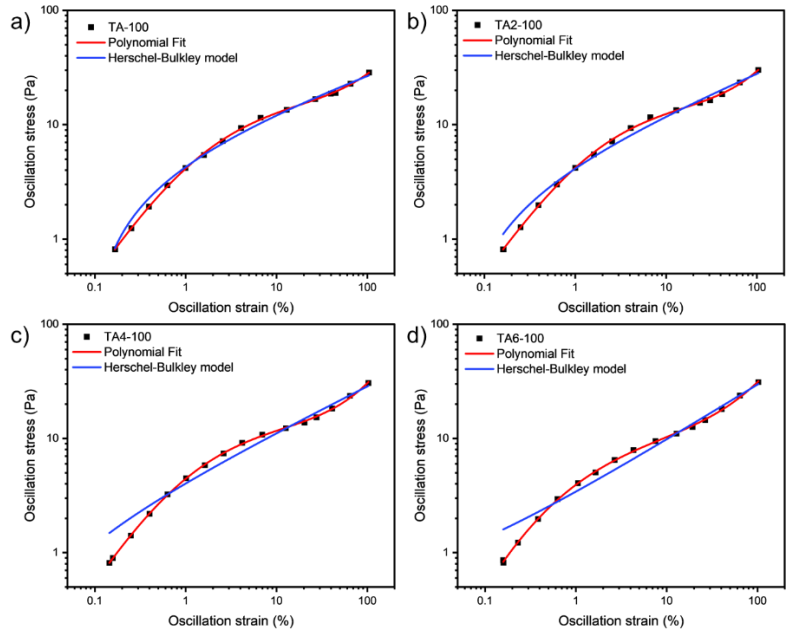

(C)

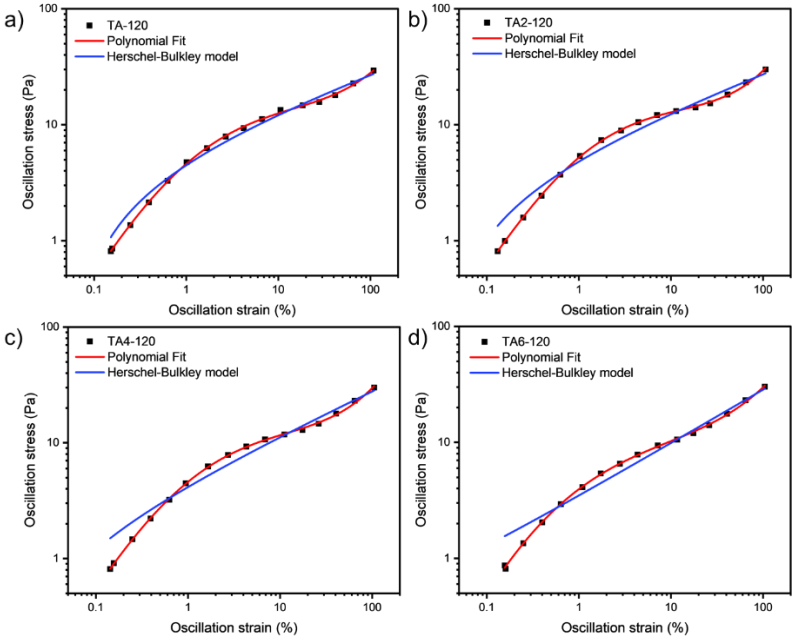

(D)

Figure 8. Oscillation strain dependence on stress of GRK-A with 0, 2, 4 and 6 wt% of LDH at different temperatures： (A) 60 ℃； (B)80 ℃； (C)100 ℃；(D)120 ℃.

Preprints (www.preprints.org) | NOT PEER-REVIEWED | Posted: 13 April 2023 doi:10.20944/preprints202304.0288.v1

Table 12. fitting parameters for different samples.

Samples	t/℃	Herschel-Bulkley				Polynomial model					
		τ_0	A(PaS)	n	R^2	τ_0	B1	B2	B3	B4	R^2
TA	60	-0.17013	5.01855	0.40503	0.97886	0.75392	0.62169	-0.30497	0.01278	0.0419	0.99969
	80	-1.40671	5.14107	0.37571	0.98927	0.59648	0.71804	-0.28236	-0.01145	0.04116	0.99982
	100	-4.57033	8.83087	0.2739	0.99217	0.61618	0.72549	-0.26076	-0.01181	0.03215	0.99973
	120	-3.69007	8.15259	0.28578	0.98624	0.66102	0.68852	-0.29324	0.00971	0.03145	0.9996
TA2	60	-0.43383	6.10031	0.38329	0.97621	0.8211	0.61639	-0.304	0.0042	0.04483	0.99975
	80	-0.40886	3.99091	0.44285	0.98991	0.58732	0.70288	-0.26138	-0.00565	0.03777	0.99978
	100	-2.55959	6.68648	0.32895	0.98663	0.62274	0.71909	-0.26752	-0.02154	0.04063	0.99956
	120	-2.83118	7.6334	0.29729	0.97754	0.71639	0.66685	-0.31873	-0.00183	0.04413	0.99967
TA4	60	-0.25301	6.2587	0.38869	0.97637	0.85047	0.6009	-0.29739	0.01151	0.04102	0.99985
	80	0.19405	3.32559	0.48983	0.99148	0.59449	0.65491	-0.2506	0.02605	0.02607	0.99981
	100	-0.73875	4.76603	0.39434	0.98524	0.64636	0.65307	-0.27959	0.01283	0.03423	0.99974
	120	-0.96712	5.10512	0.37488	0.98292	0.66186	0.64919	-0.29684	0.01464	0.03637	0.99963
TA6	60	-0.05537	6.87727	0.37931	0.97317	0.90801	0.5467	-0.28652	0.02629	0.03578	0.99985
	80	0.44239	3.20322	0.50524	0.99211	0.61746	0.61174	-0.23801	0.04488	0.01852	0.99985
	100	0.34805	3.07355	0.48968	0.99076	0.59371	0.59728	-0.26014	0.06989	0.01168	0.99965
	120	0.13685	3.35305	0.46384	0.99052	0.59669	0.59764	-0.26009	0.0638	0.01334	0.99951

3.2.2.3. Electric shovel grease viscosity and temperature analysis

The viscosity-temperature property of grease is the performance of viscosity changed by the temperature. Viscosity usually decreases with the increase of temperature. The change in viscosity of a grease is highly correlated with temperature, and there is a pattern, and the viscosity reflects the rheology of the fluid. The most commonly used equations for calculating viscosity are derived from the corresponding state or statistical principles, but this method has some limitations.

In this paper, the rheological properties of mine grease with different LDHs additions were investigated using a DISCOVERY HR-3 rotational rheometer. It can be found by Figure 9 that the viscosity changes with temperature in an approximate exponential manner, and the kinematic viscosity of the four types of grease increases sharply when cooling from 200 ℃ to -30 ℃, but the curve is relatively flat and the decline becomes smaller from 200 ℃ to 5 ℃. In the low temperature working interval (-30 ℃ to -5 ℃), the grease samples with different proportions of solid LDHs added are better than mine grease low temperature, indicating that the addition of solid LDH can change the low temperature performance of mine grease. In the high temperature working interval (40 ℃ ~ 200 ℃), the four grease samples power viscosity is comparable, indicating that after adding nano-solid LDHs, the grease in the high temperature working interval viscosity decline trend and adding three proportions of LDHs viscosity decline trend the same, especially adding 6% of LDHs viscosity slightly higher.

Preprints (www.preprints.org) | NOT PEER-REVIEWED | Posted: 13 April 2023 doi:10.20944/preprints202304.0288.v1

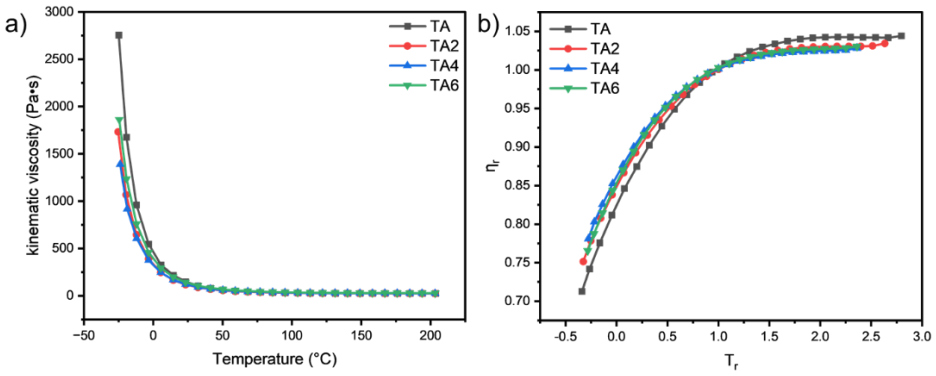

Figure 9. a) Temperature curve of different samples and b) master curves for different samples.

Further information was obtained when the viscosity data were fitted to the temperature Power Law model (Equation (4)).

$$\eta = \eta_O \left(\frac{T-T_x}{T_x}\right)^{-\gamma} \quad (4)$$

In this model, η_O represents the asymptote value, T_x is a threshold temperature at which the sample becomes fragile and γ is the parameter that modulates the effect of the temperature on the viscosity. This model allowed us to construct a master curve using the relative viscosity, η_r, and relative temperature,Tr, described by Equations (5) and (6).

$$\eta_r = \left(\frac{\eta}{\eta_o}\right)^{-1/\gamma} \quad (5)$$

$$T_r = \frac{T}{T_x} \quad (6)$$

The master curves are shown in Fig. 9b and table 13. This kind of representation has been satisfactorily used in lubricant. It is clearly seen that the addition of LDH doesn't cause a deviation in the model. LDH reduce the effect of temperature on the viscosity of the lubricant. In the case of LDH, we found a good agreement with the model as expected.

Table 13. Power Law fitting parameters for different samples.

Power Law	η_O (Pa s)	T_x (K)	γ	R^2
TA	40.65724	72.806	12.44511	0.99738
TA2	34.19674	77.234	13.72848	0.99675
TA4	33.98748	86.216	15.01109	0.99627
TA6	38.92678	86.234	14.46378	0.99768

4. Conclusion

In this paper, a new environment friendly LDHs antioxidant was developed from theoretical design and mainly through experiments. The main research contents and conclusions of this paper are as follows:

1) By XRD, IR, SEM, Laser Particle Sizer, and DSC analysis and characterization, the synthesis of lubricating oil antioxidants with excellent performance was demonstrated.

2) The synthetic LDHs was repeatedly tested and compared on different bearing lifetime tester in lithium base grease, and it was found that the environment-friendly LDHs had better performance than the traditional antioxidant, and was the development direction of a new generation of environment-friendly antioxidant in the future.

3) By adding LDHs into large electric shovel greats (GRK-A) of open pit coal mine for PDSC evaluation, it can be seen that the service lifetime of grease is extended by 20% while the overall performance of grease is not affected. Further adding different proportions of LDHs to the PDSC test, it was found that the activation energy of the four samples all met the law of ETA < ETA2 < ETA4 < ETA6 increasing, indicating that with the increase

of LDHs addition, the greater the activation energy of the reaction of grease, the stronger the resistance to thermal oxidation and decomposition.

4) Comparing the energy storage modulus and flow transition index at different temperatures, it can be seen that adding the right amount of LDHs needs close attention for the system oxidation resistance and viscoelasticity. For the electric shovel grease system, the best oxidation resistance and rheological properties can be achieved by adding 2% of LDHs. The rheological viscosity-temperature curve shows that the grease samples with different ratios of solid LDHs are better than mine grease in low temperature.

References

1. Sommer, M.; Haas, W., A new approach on grease tribology in sealing technology: Influence of the thickener particles[J]. *Tribology International* 2016, 103, 574-583.
2. Lugt, P. M., A Review on Grease Lubrication in Rolling Bearings[J]. *Tribology Transactions* 2009, 470-480.
3. Lugt, P. M., Modern advancements in lubricating grease technology[J]. *Tribology International* 2016, 97, 467-77.
4. Lisiecki, A., Tribology and Surface Engineering[J]. *Coatings* 2019, 9, 663-669.
5. Minami, I., Ionic Liquids in Tribology[J]. *Molecules* 2009,14, 2286-2305.
6. Erdemir, A., Review of engineered tribological interfaces for improved boundary lubrication[J]. *Tribology International* 2005, 38, 249-56.
7. Meghana, K. N.; Ranjtha, R.; Ganesha, A.; Suraj, P., Synthesis and characterization of size controlled nano copper oxide structures for antioxidant study and as eco-friendly lubricant additive for bio-oils[J], *Ceramics International* 2022, 49, 10402-10410.
8. Sonam, V. S.; Ganapati, D. Y., Synthesis of environment-friendly, sustainable, and nontoxic bio-lubricants: A critical review of advances and a path forward. Biofuels[J], *Bioproducts and Biorefining* 2022, 16, 1172-1195.
9. Lu Yuan, Zhan Liying, Gong Qinghai, etc. Classification, mechanism and research progress of antioxidant [J]. *Plastic Additives* 2016, 116, 43-50.
10. Brook, M. A.; Yepremyan, A.; Lu, G.; Melendez-Zamudio, M.; Hrabowyj, D. J.; Gale, C. B., Antioxidant silicone oils from natural antioxidants[J], *Green Chemistry* 2022, 24, 8751-8759.
11. Cai hongguo. Research and application status of vitamin E as polymer antioxidant [J]. *China plastics*, 2015, 29, 14-18.
12. Wen yongliang. Development and application progress of novel antioxidant [J]. *Shandong Chemical Industry* 2017, 46, 79-82.
13. Zhang, Y.; Xu, H.; Lu, S., Preparation and application of layered double hydroxide nanosheets[J]. *RSC Advances* 2021, 11, 24254-24281.
14. Xu, W.; Wang, S.; Li, A.; Wang, X., Synthesis of aminopropyltriethoxysilane grafted/tripolyphosphate intercalated ZnAl LDHs and their performance in the flame retardancy and smoke suppression of polyurethane elastomer[J]. *RSC Advances* 2016, 6, 48189-48198.
15. Dragoi, B.; Uritu, C. M.; Agrigoroaie, L.; Lutic, D.; Hulea, V.; Postole, G.; Coroaba, A.; Carasevici, E., MnAl-Layered Double Hydroxide Nanosheets Infused with Fluorouracil for Cancer Diagnosis and Therapy[J]. *ACS Applied Nano Materials* 2021, 4, 2061-2075.
16. Jiang, Y.; Yang, Z.; Su, Q.; Chen, L.; Wu, J.; Meng, J., Preparation of Magnesium-Aluminum Hydrotalcite by Mechanochemical Method and Its Application as Heat Stabilizer in poly (vinyl chloride) [J]. *Materials* 2020, 13, 5223-5238.
17. Wang X B, Bai Z M, Zhao D, Zhao F Y. Friction behavior of Mg–Al–CO3 layered double hydroxide prepared by magnesite[J]. *Applied Surface Science* 2013, 277, 134-138.
18. Kuang, Y.; Zhao, L.; Zhang, S.; Zhang, F.; Dong, M.; Xu, S. Morphologies, Preparations and Applications of Layered Double Hydroxide Micro-/Nanostructures[J]. *Materials* 2010, 3, 5220-5235.
19. Meszáros, S.; Halász, J.; Kónya, Z.; Sipos, P.; Pálinkó, I.Reconstruction of Calcined MgAl- and NiMgAl-Layered Double Hydroxides during Glycerol Dehydration and Their Recycling Characteristics[J]. *Applied Clay Science* 2013, 80-81.
20. Wang H D, Liu Y H, Liu W R, Wang R, Wen J G, Sheng H P, Peng J F, Erdemir A, Luo J B. Tribological behavior of NiAl-Layered double hydroxide nanoplatelets as oil-based lubricant additives[J]. *ACS Applied Materials & Interfaces* 2017, 9, 30891-30899.
21. Wang H D, Liu Y H, Liu W R, Liu Y M, Wang K P, Li J J, Ma T B, Eryilmaz O L, Shi Y J, Erdemir A, et al. Superlubricity of polyalkylene glycol aqueous solutions enabled by ultrathin layered double hydroxide nanosheets[J]. *ACS Applied Materials & Interfaces* 2019, 11, 20249-20256.
22. Malak-Polaczyk A, Vix-Guterl C, Frackowiak E. Carbon/ Layered Double Hydroxide (LDH) composites for super capacitor application[J]. *Energy Fuels* 2010, 24, 3346-3351.
23. Ma W, Ma R Z, Wang C X, Liang J B, Liu X H, Zhou K C, Sasaki T. A superlattice of alternately stacked Ni–Fe hydroxide nanosheets and graphene for efficient splitting of water[J]. *ACS Nano* 2015, 9, 1977-1984.
24. O'Leary S, O'Hare D, Seeley G. Delamination of layered double hydroxides in polar monomers: new LDH-acrylate nanocomposites[J]. *Chemical Communications* 2002, 14, 1506-1507.
25. Wang Lijuan, Liu Weimin. Mechanism of lubricating oil antioxidant [J]. *Lubricating oil* 1998, 13, 55-58.